

Long-term device stability for Raman spectroscopy

Shuxia Guo^{1,2*}, Anuradha Ramoji^{1,2}, Aikaterini Pistiki^{1,2}, Yilmaz Hulya^{1,2}, Uwe Glaser^{1,2}, David L Vasquez-Pinzon^{1,2}, Iwan Schie^{1,2}, Ute Neugebauer^{1,2,3}, Anja Silge^{1,2}, Jürgen Popp^{1,2}, Thomas Bocklitz^{1,2}

¹Leibniz Institute of Photonic Technology, Member of Leibniz Health Technologies, Member of the Leibniz Centre for Photonics in Infection Research (LPI), Albert-Einstein-Strasse 9, 07745 Jena, Germany.

²Institute of Physical Chemistry (IPC) and Abbe Center of Photonics (ACP), Friedrich Schiller University Jena, Member of the Leibniz Centre for Photonics in Infection Research (LPI), Helmholtzweg 4, 07743 Jena, Germany.

³Center for Sepsis Control and Care (CSCC), Jena University Hospital, Am Klinikum 1, 07745, Jena, Germany.

Correspondence: shuxia.guo@uni-jena.de

Information of measured substances

Liquid

- Benzonitrile: Sigma. #Cat.: 8.01800, Lot: S8127400204, European Pharmacopoeia (EP) reference standard
- Cyclohexane purity $\leq 99,9\%$: Sigma. #Cat.: 650455, Lot: 4503599040, European Pharmacopoeia (EP) reference standard
- Isopropanol: $\leq 99\%$: VWR: 0981-1L
- DMSO anhydrous, purity 99,9%: Sigma. #Cat.: 276855, Lot: 102507742, European Pharmacopoeia (EP) reference standard
- Ethanol BioUltra pure $\leq 99,8\%$: Sigma-Aldrich, Taufkirchen, Germany. #Cat.: 51976, Lot: 102462317, European Pharmacopoeia (EP) reference standard
- Squalane purity $\leq 95\%$: Sigma. #Cat.: 85630, Lot: 102548224, European Pharmacopoeia (EP) reference standard
- Squalene purity $\leq 98\%$: Sigma. #Cat.: S3626, Lot: 1003407418, European Pharmacopoeia (EP) reference standard

Solid

- Polystyrene: NIST certified reference standard, Polystyrene Rod Standard, Rigaku, Neu-Isenburg, Germany. #Cat.: 1030497, Lot.Nr.: J29474
- Silicon wafers

Powder

- Paracetamol (4AAP), purity 98-102%: Sigma. Cat.: A5000, Lot MKBS7142V
- Sucrose, BioUltra pure $\leq 99,5\%$: Sigma. #Cat.: 84097, Lot: 102497831, European Pharmacopoeia (EP) reference standard
- D-(-)-Fructose BioUltra pure $\leq 99\%$: Sigma. #Cat.: 47739, Lot: 102501951, European Pharmacopoeia (EP) reference standard
- D-(+)-Glucose monohydrate purity $\leq 99\%$: Sigma. Cat.: 49159, Lot: 102473227, European Pharmacopoeia (EP) reference standard

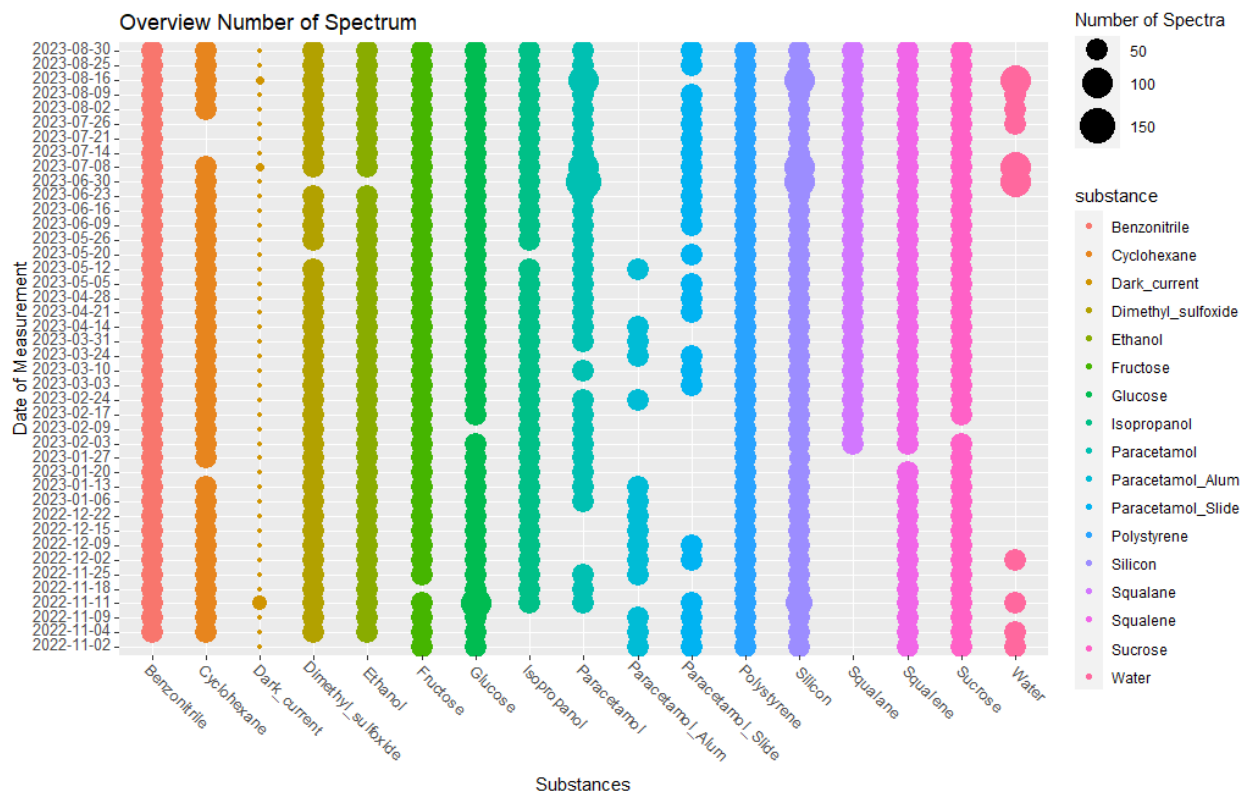


Figure S1. Overview of the data size for each substance and each measurement day. It is worth to mention that not all substances were measured over the whole period, for instance squalane, paracetamol-alum, and water.

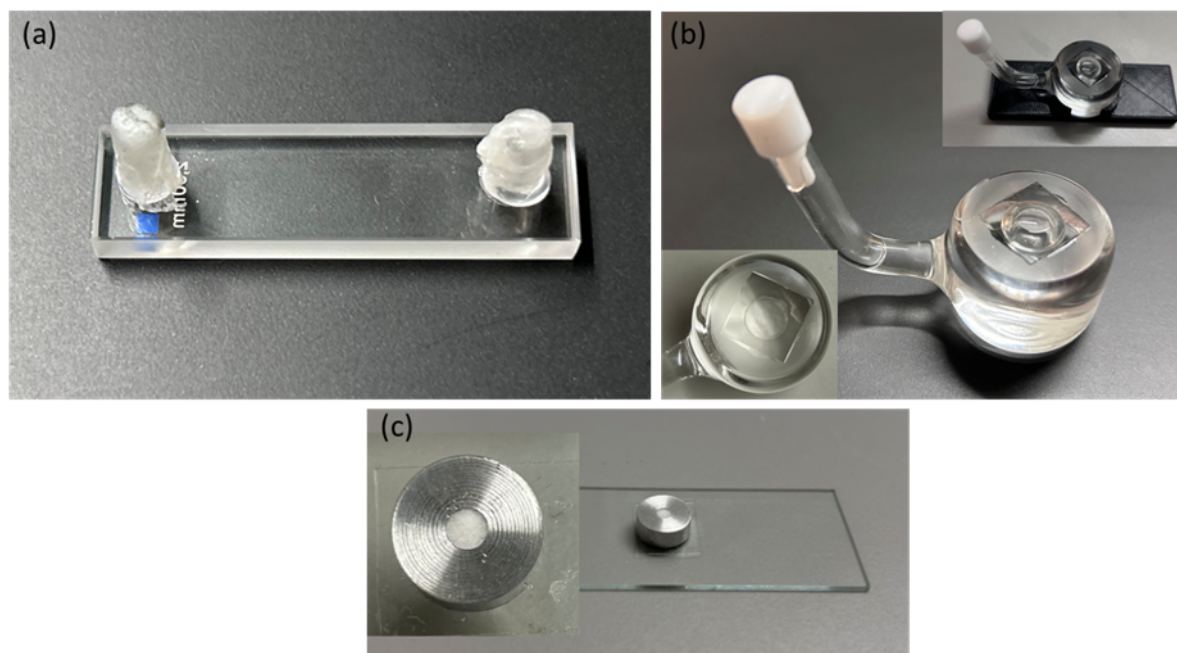


Figure S2. Images of sample holders. (a) The quartz glass flow cell with a 520 μL volume (Helma, model 137-QS, 6349813) was utilized for squalene and squalane. It features a 2 mm layer thickness, 45 mm height, 12.5 mm width, and 4.5 mm depth. (b) The 12x12 mm cuvette is used for DMSO, Benzonitrile, Isopropanol, Ethanol, cyclohexane. It is made of glass and covers a 200 μm thick quartz on top. It has a cut-out section for easy filling, and a Teflon plug securely seals the opening, keeping the sample inside intact. (c) aluminum holder was used for pressed Paracetamol, Fructose, Glucose, and Sucrose. They were produced in the Institute of Physical Chemistry at Friedrich Schiller University's workshop. They consist of slices cut from an aluminum cylinder, each featuring a drilled hole.

spectra

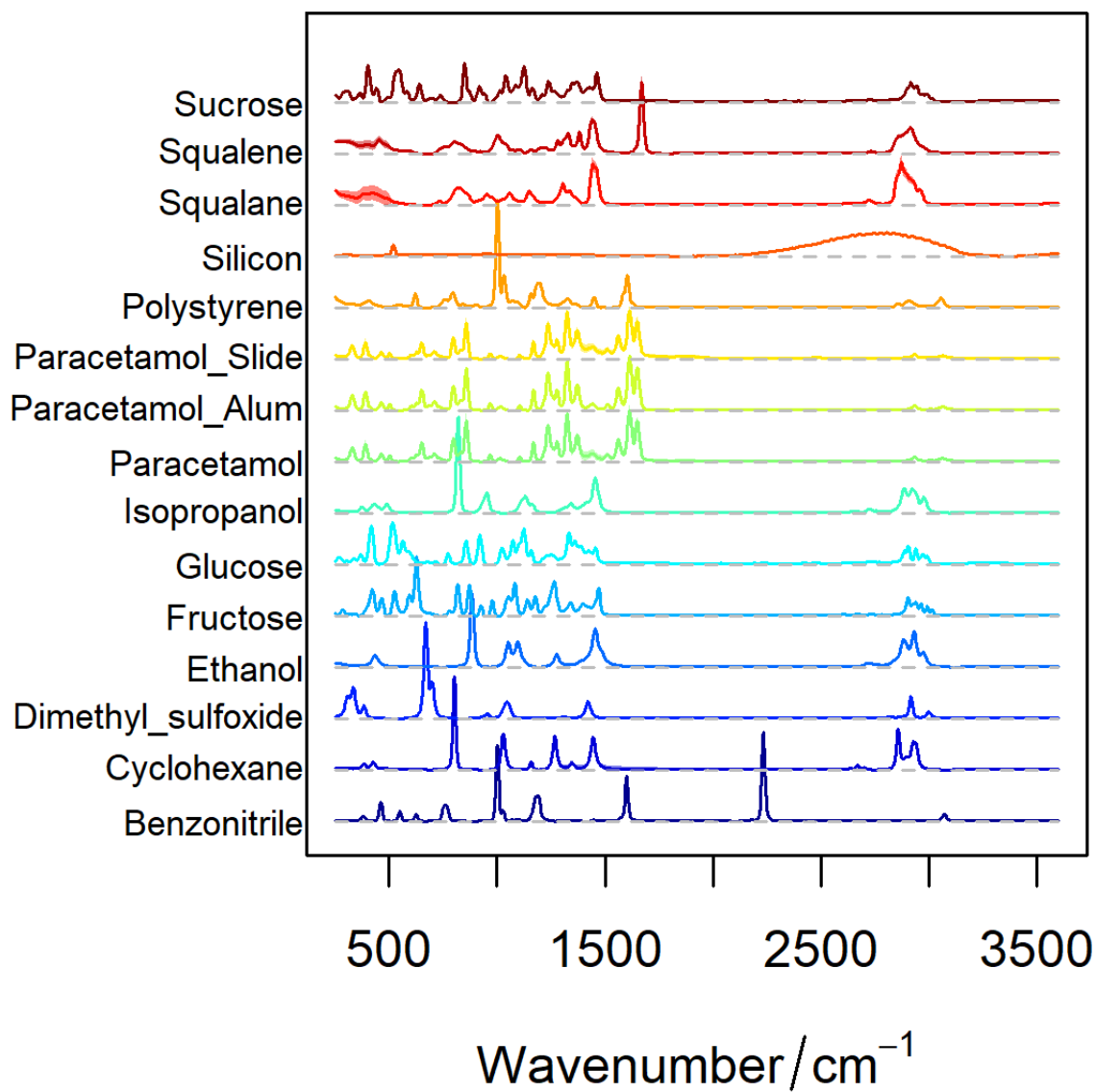


Figure S3. Mean spectra and standard deviation for each substance over all measurement days. The spectra from dark current and water are not shown as they do not contain clear Raman band that are essential for the analysis in this study.

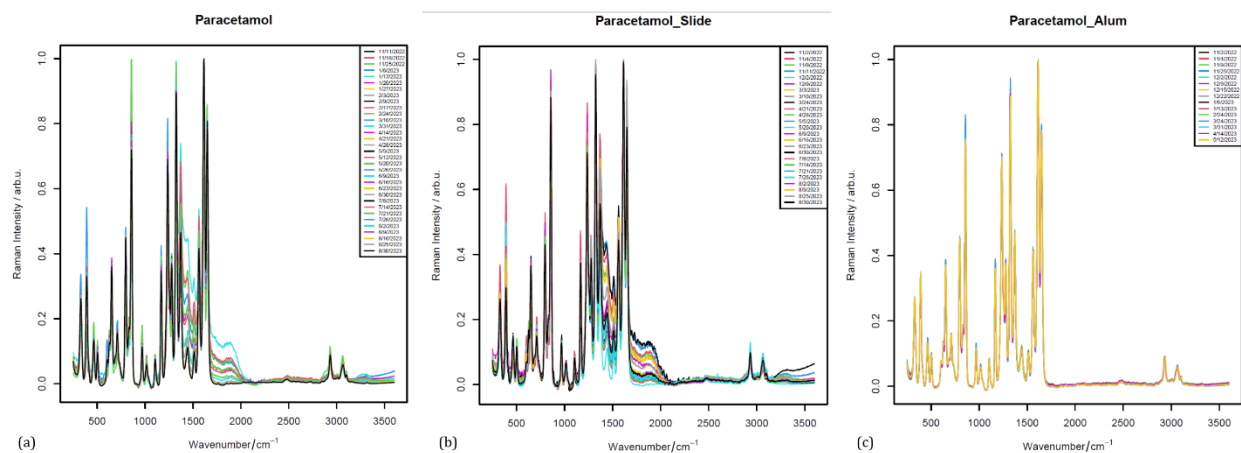


Figure S4. Comparison of spectra from paracetamol measured on different substrates. The measurement on slide (a-b) showed severe variations caused by the focusing instability, while those on the aluminum film (c) are quite stable.

Cyclohexane

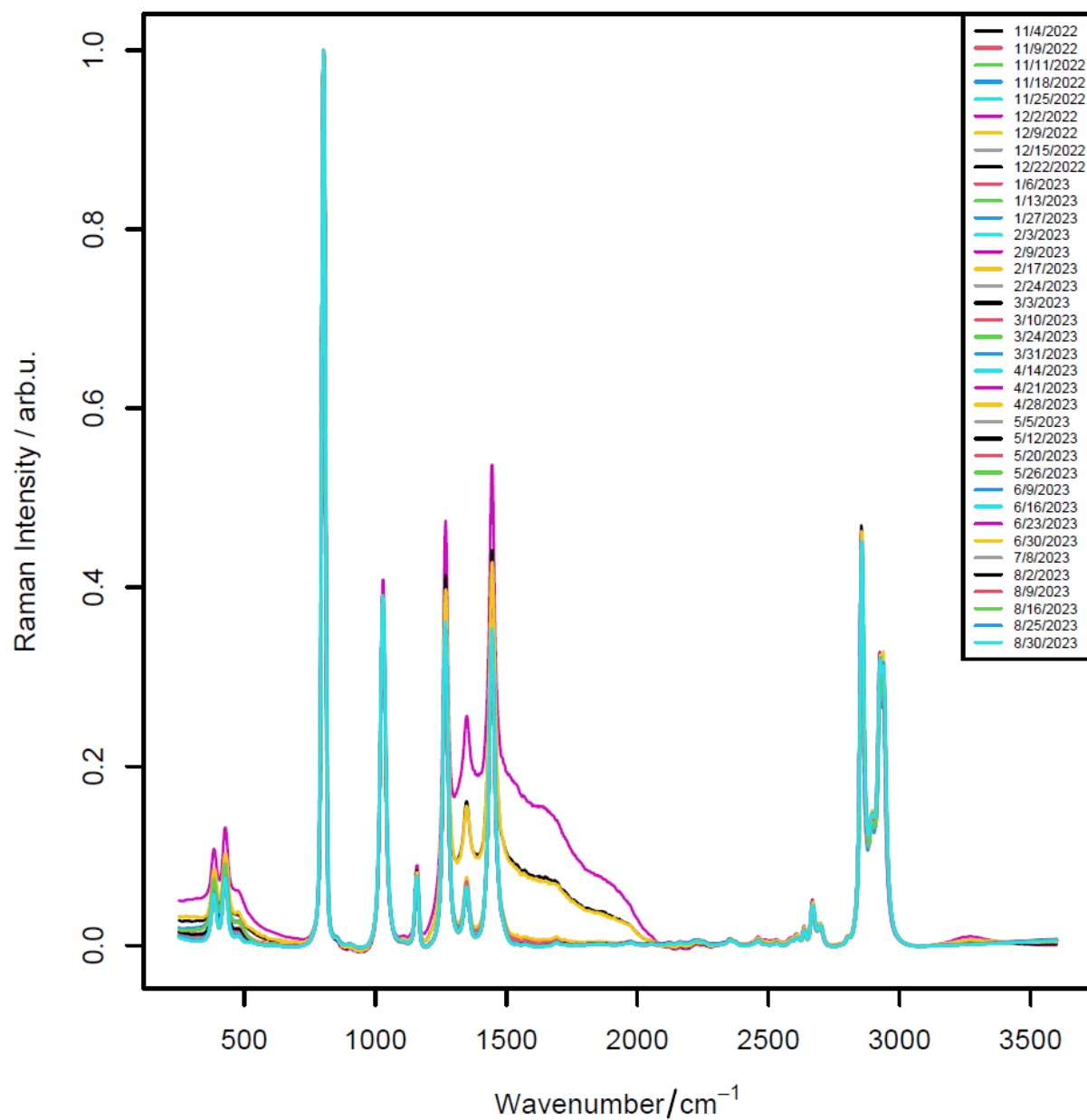


Figure S5. Spectra from cyclohexane, which shows contamination during the measurement.

Squalane

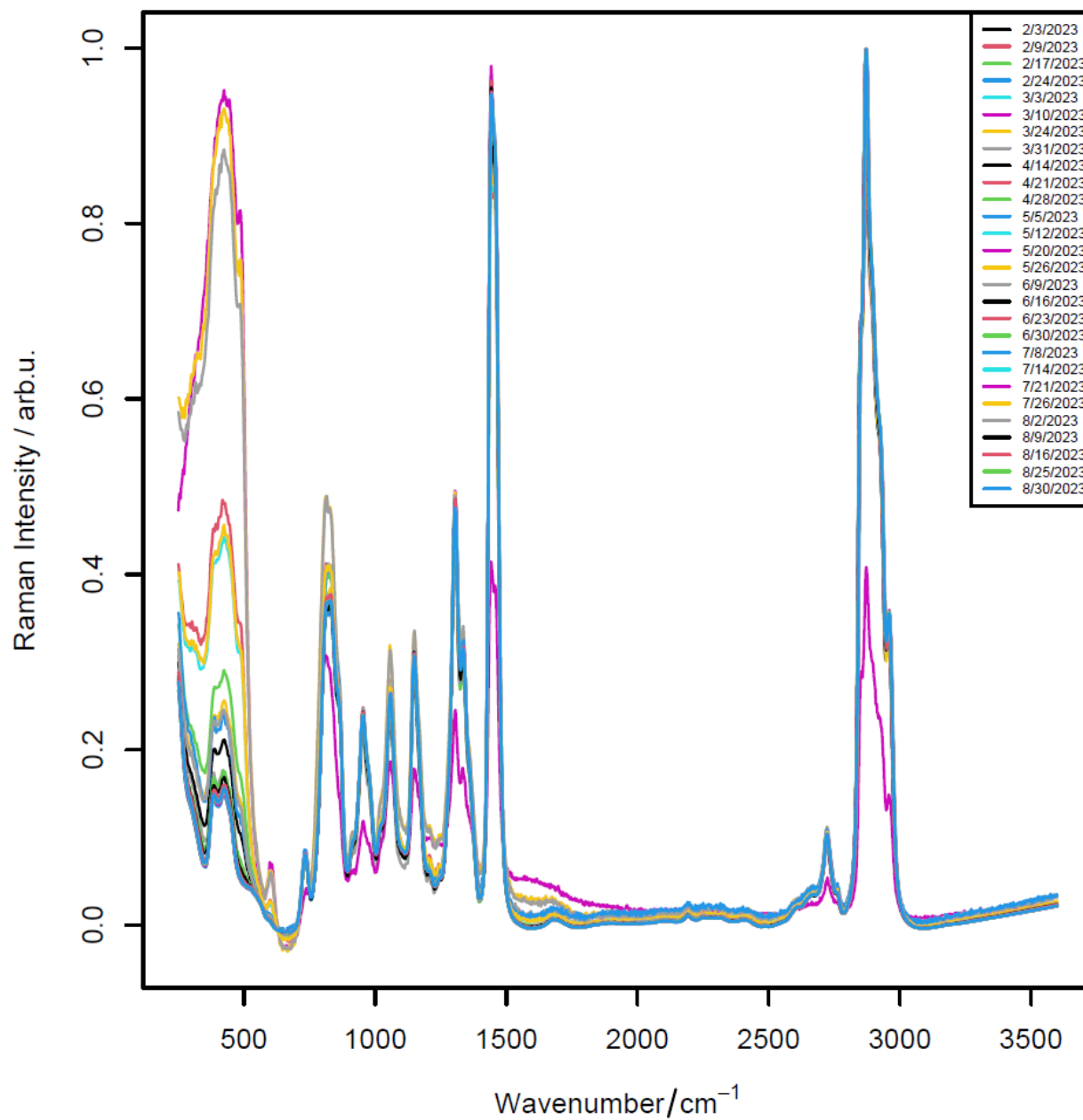


Figure S6. Spectral from squalane, which show instability for spectral range below 500 cm⁻¹.

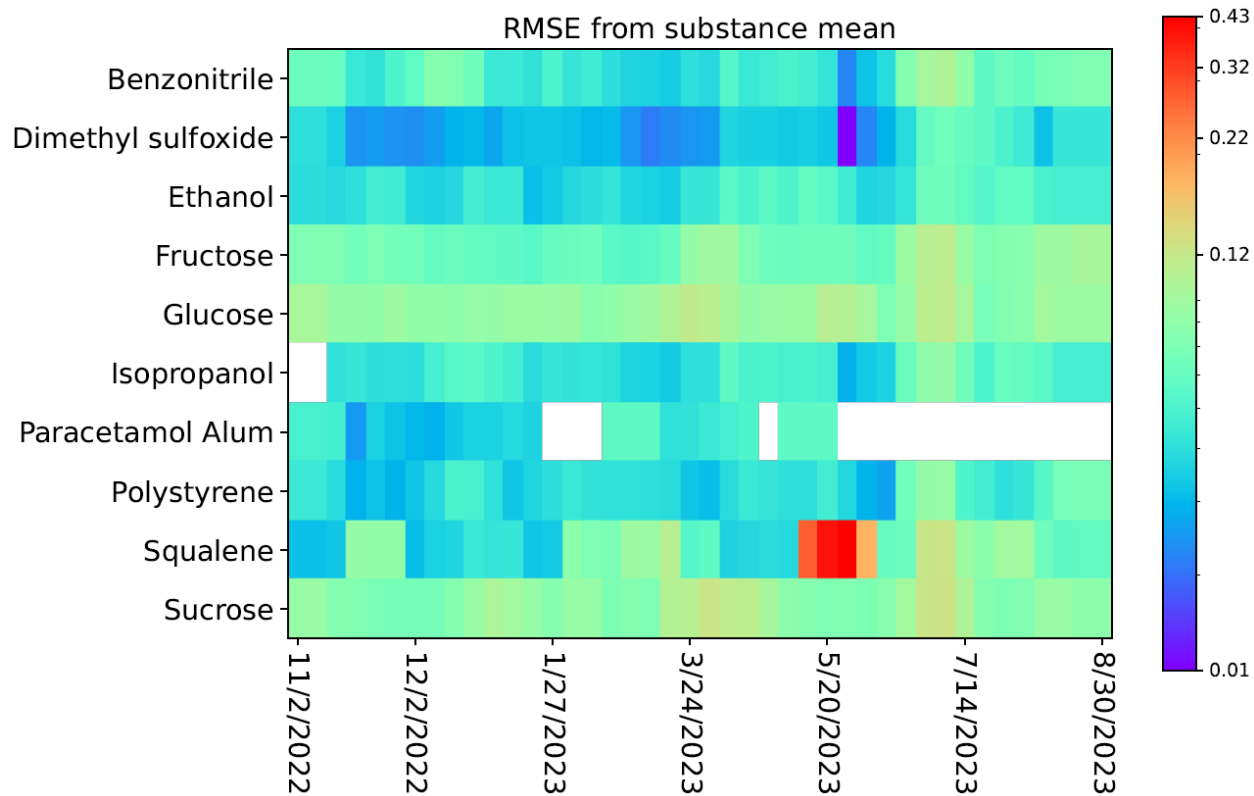


Figure S7. Results of the RMSE calculated from the move-window strategy. Missing data are visualized as white color.

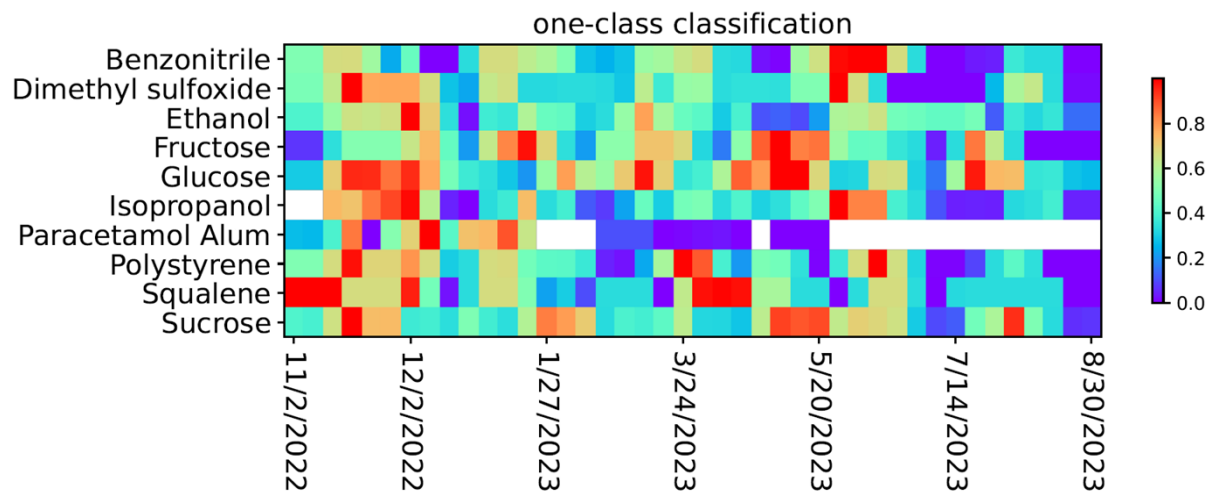


Figure S8. Accuracy results of the one-class classifications in move-window mode.

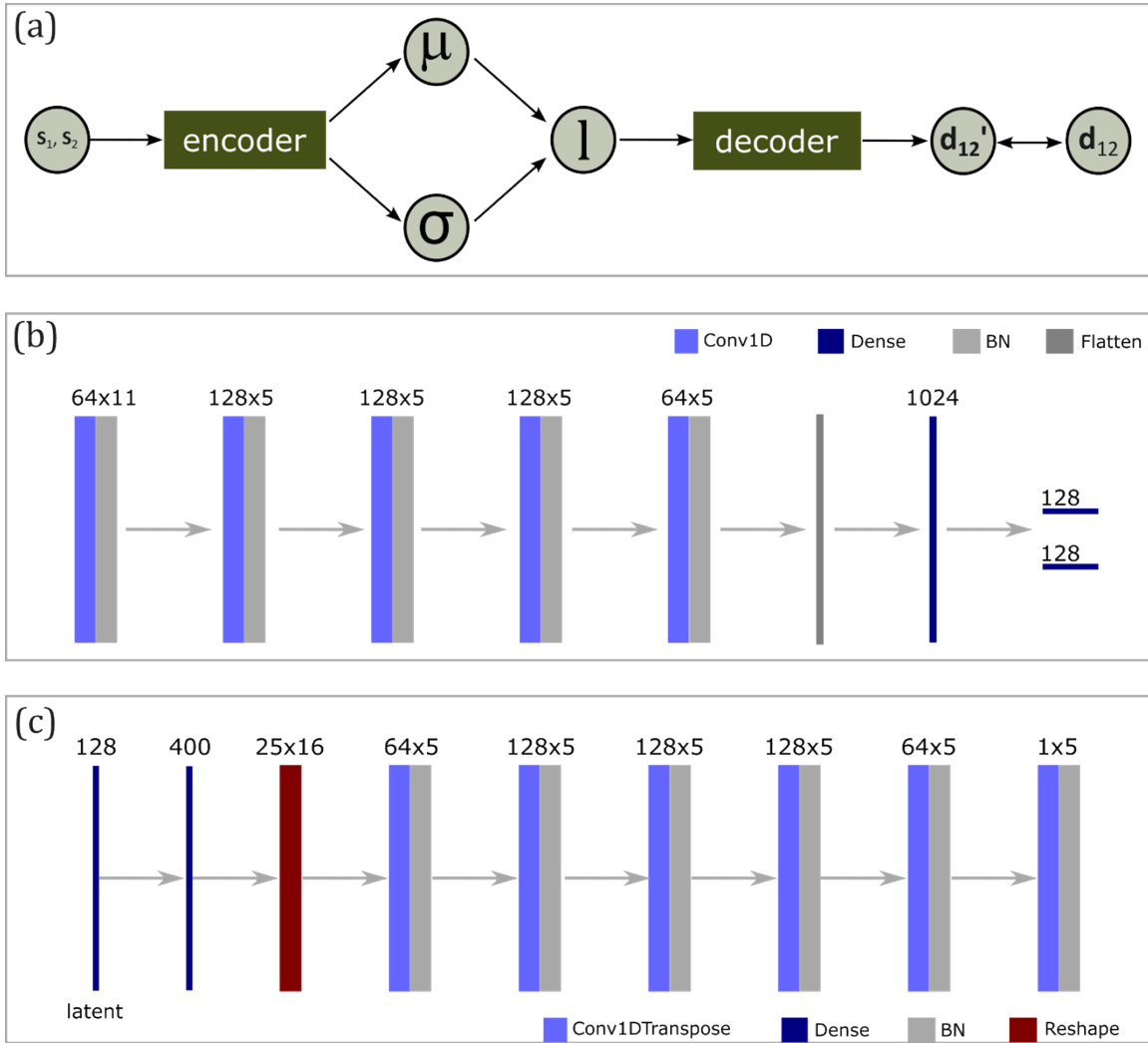


Figure S10. The architecture of the variational autoencoder (VAE). (a) The structure of the VAE network, which is composed of an encoder and decoder. The encoder accepts a spectral pair (s_1, s_2) as input and outputs a latent space represented by mean (μ) and variance (σ). A latent vector is then sampled from the latent space, which was used by the decoder to obtain the difference spectrum between s_1 and s_2 . (b) Architecture of the encoder, which consists of five convolutional layers and two fully connected layers to embed an input spectral pair (s_1, s_2) into two vectors of 128 features, representing the mean and variance of the latent space, respectively. A stride of 2 was used for all convolutional layers. (c) Architecture of the decoder, which takes latent vector as input, followed by a dense layer, a reshape layer and six transposed convolutional layers to output the difference spectrum between s_1 and s_2 . A stride of 2 was used for all except the last convolutional layers. In panels (b-c), the number and kernel size of the filters for each convolutional layer were remarked in the format of ($n_{filter} \times size_{kernel}$). The values marked above the other layers represent the output shape of this layer.

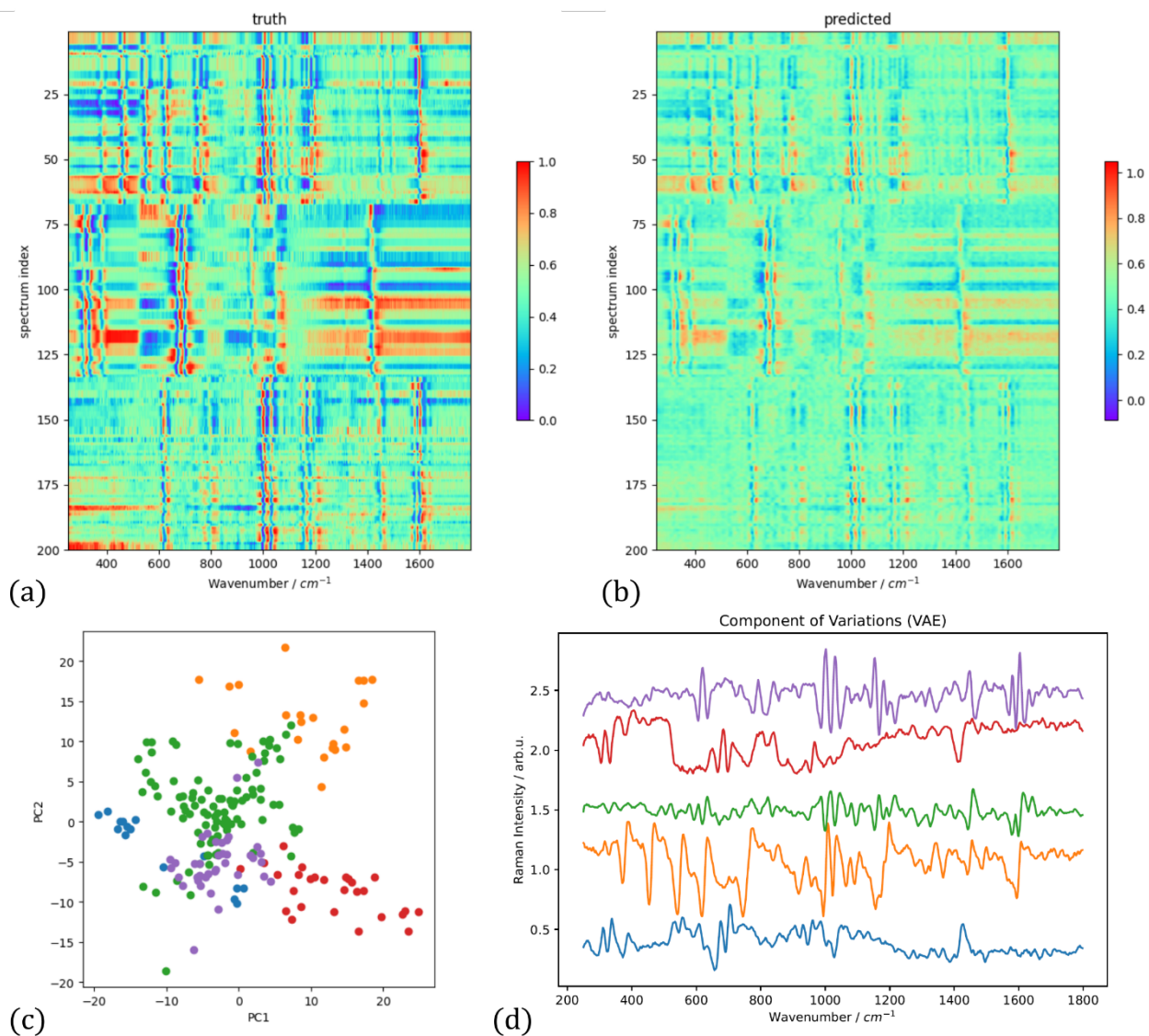


Figure S11. Results of VAE. (a-b) Ground truth and the prediction of the VAE model. (c) Results of the clustering conducted on the latent vectors, which were the output of the trained encoder on the 200 testing spectral pairs. Each dot corresponds to one spectral pair. The five clusters are visualized by five colors. (d) The output of the trained decoder taking input of the latent vectors that are the closest to the centroid for all clusters in (c).

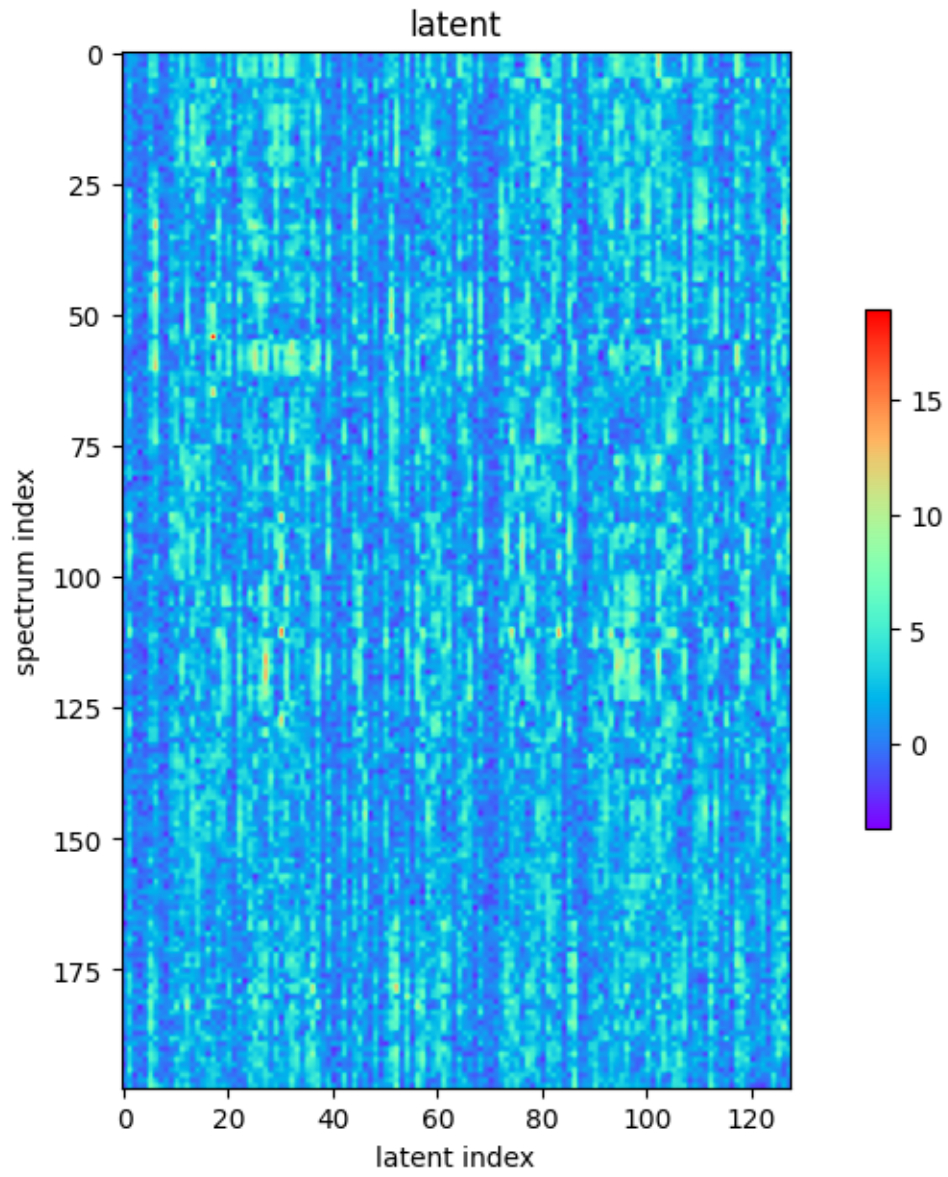


Figure S12. Results of latent vectors on test data.

Spectral preprocessing

All spectra were preprocessed following a pipeline of de-spiking, wavenumber calibration, baseline correction, and normalization. Particularly, the de-spiking was achieved via a pairwise comparison, i.e., to detect spikes as abnormally intensive differences (outside of $\mu \pm 10\sigma$) between two successively measured spectra of the same substance and remove each spike via a linear interpolation between its starting and ending wavenumber points. For wavenumber calibration, the shifts on the wavenumber axis was estimated as 3-order polynomial fitted from the shifts in well-defined peaks of the standard reference. The shifts of peaks from all standards were combined and ordered according to the peak position before polynomial fitting in case of multi-standard calibration. Thereafter, the baseline was corrected by the SNIP method (C.G. Ryan et al., Nuclear Instruments and Methods in Physics Research Section B, 1988), with the parameter of iterations=40. All spectra were cut-off to remain spectral region of wavenumber < 1800 cm^{-1} , followed by a vector normalization.

VAE

To estimate the spectral variations over-time, we established a method in combination with Variational autoencoders (VAE) and extensive multiplicative scattering correction (EMSC). The VAE was employed to estimate the spectral variations, which were input into EMSC to suppress these variations from the measured data. Details of VAE and EMSC are given as follows.

VAE is a variant of autoencoder, which is composed of an encoder and a decoder. However, instead of learning a single-point latent representative for each input data, the encoder in VAE learns a distribution of the latent space characterized by *mean* and *variance*. A latent representative is re-sampled from this distribution and used as input of the decoder for reconstruction. Normally, the encoded distribution is enforced to follow a standard normal distribution, which is achieved by introducing a Kullback-Leibler (KL) divergence into the loss function of the network.

In our study, we adapted the VAE architecture to accept input of spectral-pairs and output the difference spectrum of each pair. The architecture of the network is shown in Figure S10 (a), which takes a spectral pair (s_1, s_2) as input and outputs the difference spectrum between s_1 and s_2 . The Encoder and a Decoder are depicted in Figure S10(b-c). The Encoder takes a spectral pair (s_1, s_2) as input and outputs a latent space represented by mean (μ) and variance (σ). A latent vector is then sampled from the latent space, which was used by the Decoder to obtain the difference spectrum between s_1 and s_2 . The Encoder consists of five convolutional layers and two fully connected layers to embed an input spectral pair (s_1, s_2) into two vectors of 128 features, representing the mean and variance of the latent space, respectively. A stride of 2 was used for all convolutional layers. The Decoder takes latent vector as input, followed by a dense layer, a reshape layer, and six transposed convolutional layers to output the difference spectrum between s_1 and s_2 . A stride of 2 was used for all except the last convolutional layers. The number and kernel size of the filters for each convolutional layer were remarked in Figure S10(b-d) in the

format of $(n_{filter} \times size_{kernel})$. The values marked above the other layers represent the output shape of this layer.

EMSC

The idea of EMSC can be formulated with Eq. S1a-b, in which the input spectrum $I(\tilde{\nu})$ is modeled as a reference spectrum $m(\tilde{\nu})$ together with the polynomials of order n , the interference component $p_k(\tilde{\nu})$, and the residual $e(\tilde{\nu})$. The parameters a , b , and g are obtained via a least squares fitting, after which the contributions of the polynomials and interferences are removed via Eq. S1b to obtain the corrected spectrum. Among these the polynomials represent the slowly changing baseline beneath the spectral peaks, the interferences can be components representing the contributions that need to be removed. In our study, we used the resulting spectral variations from VAE as the interference.

$$I(\tilde{\nu}) = a + b \cdot m(\tilde{\nu}) + d_1 \tilde{\nu} + d_2 \tilde{\nu}^2 + \dots d_n \tilde{\nu}^n + \sum_{k=1}^N g_k \cdot p_k(\tilde{\nu}) + e(\tilde{\nu}) \quad (S\ 1a)$$

$$I_c(\tilde{\nu}) = \left(I(\tilde{\nu}) - a - d_1 \tilde{\nu} - d_2 \tilde{\nu}^2 - \dots d_n \tilde{\nu}^n - \sum_{k=1}^N g_k \cdot p_k(\tilde{\nu}) \right) / b \quad (S\ 1b)$$